PHYSICAL REVIEW C **88**, 035501 (2013)

# Polarization of the neutron induced by hadronic weak interactions in the photodisintegration of the deuteron

J. W. Shin,[1] C. H. Hyun,[2,3,*] S.-I. Ando,[2] and S. W. Hong[4]

[1]*Department of Physics, Sungkyunkwan University, Suwon 440-746, Korea*

[2]*Department of Physics Education, Daegu University, Gyeongsan 712-714, Korea*

[3]*School of Physics, Korea Institute for Advanced Study, Seoul 130-722, Korea*

[4]*Department of Physics and Department of Energy Science, Sungkyunkwan University, Suwon 440-746, Korea*

(Received 12 March 2013; revised manuscript received 13 July 2013; published 3 September 2013)

New polarization observables with which we can study the two-nucleon weak interactions at low energies are considered. In the breakup of the deuteron by photons, polarization of outgoing neutrons can depend on the parity-violating component of two-nucleon interactions. We express the parity-violating polarization in general forms, and perform numerical calculations with a pionless effective field theory. The theory has three unknown parity-violating low energy constants, and new polarization observables are expressed in linear combinations of them. We discuss how the unknown constants may be determined and their implication to the understanding of the hadronic weak interactions.

DOI: 10.1103/PhysRevC.88.035501 PACS number(s): 13.75.Cs, 14.20.Dh, 24.70.+s, 24.80.+y

## I. INTRODUCTION

The present understanding about the most fundamental interactions is that parity is not conserved only in the weak interactions. Such a nature of the weak interaction has been successfully probed in leptonic and semileptonic processes in high-energy experiments as well as in radioactive decays. In principle, parity-violating (PV) aspects of the weak interaction can emerge in the pure hadronic processes too at both high and low energies. However our understanding of PV aspects of the weak interaction in the low energy region is still very poor even though more than 50 years have passed since the first observation of the parity violation in nuclear phenomena.

Nevertheless, efforts in both experiments and theories have been continued. Especially there has been significant progress in the low energy few-nucleon systems in the last three decades. In Ref. [1], the authors wrote down the two-nucleon PV interactions in terms of $\pi$-, $\rho$-, and $\omega$-meson exchanges (so-called DDH potential), which contain seven weak meson-nucleon coupling constants. Several PV observables in nuclear and hadronic processes have been calculated in terms of the DDH potential, and experiments were attempted to determine the values of the seven weak meson-nucleon coupling constants. In the last decade, calculations have been improved by using modern nucleon-nucleon (*NN*) phenomenological potentials such as Argonne v18, CD Bonn, and Nijmegen93. Relevant PV observables are the asymmetry of the photon momentum with respect to the neutron spin in $\vec{n}p \to d\gamma$ [2,3], the anapole moment of the deuteron [4,5], several quantities in elastic $e-d$ scattering [6], polarization in $np \to d\gamma$ [7] or asymmetry in $d\vec{\gamma} \to np$ [8–10] due to the circularly polarized photons, and the longitudinal asymmetry in $\vec{p}p$ scattering [11,12]. The PV observables were expressed in terms of the seven meson-nucleon coupling constants in the DDH potential. Longitudinal asymmetries were measured with good accuracies at low energies [13]. PV circular polarization of the $\gamma$ ray in $np \to d\gamma$ was measured in the late 1970s, but the experiments could provide only the upper limit [14]. PV up-down asymmetry $A_\gamma$ with respect to the neutron spin direction of $\gamma$ rays emitted from $\vec{n}p \to d\gamma$ is under measurement at SNS in Oak Ridge [15], and there was an experimental trial for the measurement of the deuteron anapole moment.

In the meantime, there was a reformulation of the theory for the PV interactions in the framework of effective field theory (EFT) [16]. The authors in Ref. [16] derived the *NN* PV interactions from a theory with pions (pionful theory) and also without pions (pionless theory). In the pionless theory where all the interactions are described in terms of contact terms only, it was shown that only five PV low energy constants (LECs) are independent after removing redundancy in the DDH potential [17]. PV observables in the two-nucleon systems were recalculated with the EFT PV potentials with and without pions [18–23]. Nowadays, determination of the PV LECs in the pionless theory is getting more attention in the field. Asymmetry in $d\vec{\gamma} \to np$ is now becoming a potential candidate for the measurements in the two-nucleon processes. Measurements have been proposed at JLab, SPring-8, Shanghai Synchrotron, and most recently at TUNL. The aimed accuracy in the experiment at TUNL is of the order of $10^{-8}$, with which one can obtain stringent constraint to pin down the values of either meson-nucleon coupling constants in the DDH potential or the PV LECs in the pionless theory. For precise determination of the coupling constants or LECs, however, it is necessary to have additional observables.

In this work, we calculate polarization of the neutron in $d\gamma \to \vec{n}p$ at low energies. There is a long history of discrepancy between theory and experiment for the polarization $P_{y'}$ [24–28], which is a parity-conserving (PC) quantity. This problem of discrepancy was revisited by using a pionless EFT with dibaryon fields as auxiliary fields for the two-nucleon states [29]. With dibaryon fields, the calculation becomes simple and the convergence is especially efficient at low

*hch@daegu.ac.kr

 

energies. In fact, we applied the theory successfully to various quantities such as the electromagnetic moments of the deuteron [30], $np$ capture at the big-bang nucleosynthesis energies [31], and $pp$ fusion in the Sun [32]. Though we observed good agreement with other theoretical results for $P_{y'}$ at low energies by using dibaryons, the discrepancy with the measurements still remains unresolved. $P_{y'}$ is the polarization along the $y'$ axis (convention for the coordinate system will be shown later). One can also think of the polarization along $z'$ and $x'$ directions, but they vanish if only PC interactions are considered. As will be shown in the following section, however, PV interactions cause nonzero contributions to $P_{z'}$ and $P_{x'}$. Motivated by this simple observation, we calculate $P_{z'}$ and $P_{x'}$ with a pionless EFT with dibaryon fields. By assuming the first order approximation, the observables are obtained in the linear combination of PV LECs. Since the values of PV LECs are completely unknown, we cannot determine the numerical values of the polarizations. Instead, the coefficients for the PV LECs can be calculated easily. We compare the resultant coefficients with those appearing in other PV observables such as the asymmetry in $\vec{n}p \to d\gamma$ and the polarization in $np \to d\gamma$. Through this comparison, we can roughly estimate the order of the physical quantities, and discuss the feasibility of the measurements.

The paper is organized as follows. In Sec. II, we present the basic Lagrangians. In Sec. III, we obtain the diagrams and calculate the amplitudes up to the next-to-leading order (NLO). The numerical results are discussed in Sec. IV. We summarize the work in Sec. V, and detailed forms of complicated equations are given in the Appendix.

## II. EFFECTIVE LAGRANGIAN

In the pionless theory, pions are treated as heavy degrees of freedom, and thus the typical scale of expansion parameter is $Q/m_\pi$, where $Q$ is a physical or exchange momentum. In a system where scattering length is unusually long or binding energy is very shallow, one can also treat these small scales as expansion parameters. It is natural to assign order $Q$ to the quantities such as $\gamma$, $1/a_0$, $1/a_1$, $1/r_0$, and $1/\rho_d$, where $a_0$, $a_1$ are the $np$ scattering length in the ${}^1S_0$ and ${}^3S_1$ states, respectively, and $r_0$ is the effective range in the ${}^1S_0$ state. $\gamma = \sqrt{m_N B}$ where $B$ is the binding energy of the deuteron and $\rho_d$ is the effective range corresponding to the deuteron. In a diagram, propagators of a single nucleon and a dibaryon field are counted as $Q^{-2}$ and the integration of a nucleon loop generates $Q^5$.

### A. Parity-conserving part

PC part of the Lagrangian consists of strong and electromagnetic (EM) interactions. PC Lagrangian with dibaryon fields can be written as [30]

$$\mathcal{L}_{\rm PC} = \mathcal{L}_N + \mathcal{L}_s + \mathcal{L}_t + \mathcal{L}_{st}, \tag{1}$$

where $\mathcal{L}_N$, $\mathcal{L}_s$, $\mathcal{L}_t$, and $\mathcal{L}_{st}$ include interactions for nucleons, dibaryon in ${}^1S_0$ state, dibaryon in ${}^3S_1$ state, and EM transition between ${}^1S_0$ and ${}^3S_1$ states, respectively. Retaining terms that are relevant to the present work, we have

$$\mathcal{L}_N = N^\dagger \left\{ iD_0 + \frac{\vec{D}^2}{2m_N} - \frac{e}{2m_N}\frac{1}{2}(\mu_S + \mu_V \tau_3)\vec{\sigma}\cdot\vec{B} \right\} N, \tag{2}$$

$$\mathcal{L}_s = -s_a^\dagger \left\{ iD_0 + \frac{\vec{D}^2}{4m_N} + \Delta_s \right\} s_a - y_s\left\{ s_a^\dagger \left[ N^T P_a^{({}^1S_0)} N\right] + \text{H.c.}\right\}, \tag{3}$$

$$\mathcal{L}_t = -t_i^\dagger \left\{ iD_0 + \frac{\vec{D}^2}{4m_N} + \Delta_t \right\} t_i - y_t\left\{ t_i^\dagger \left[ N^T P_i^{({}^3S_1)} N\right] + \text{H.c.}\right\} - \frac{2L_2}{m_N \rho_d}(i)\epsilon_{ijk} t_i^\dagger t_j B_k, \tag{4}$$

$$\mathcal{L}_{st} = \frac{L_1}{m_N\sqrt{r_0\rho_d}}[t_i^\dagger s_3 B_i + \text{H.c.}], \tag{5}$$

where the projection operators for the ${}^1S_0$ and ${}^3S_1$ states are respectively defined as

$$P_a^{({}^1S_0)} = \frac{1}{\sqrt{8}}\sigma_2\tau_2\tau_a, \quad P_i^{({}^3S_1)} = \frac{1}{\sqrt{8}}\sigma_2\sigma_i\tau_2. \tag{6}$$

The covariant derivative is defined as $D_\mu \equiv \partial_\mu - ieq\mathcal{V}_\mu^{\rm ext}$ where $\mathcal{V}_\mu^{\rm ext}$ represents the external vector field. For the nucleon, we use $D_0 = \partial_0 - ieq\mathcal{V}_0^{\rm ext}$ and $\vec{D} = \vec{\nabla} + ieq\vec{\mathcal{V}}^{\rm ext}$, where $q = \frac{1}{2}(1+\tau_3)$ is the charge operator. For the dibaryon fields, we have $D_0 = \partial_0 - ie\mathcal{V}_0^{\rm ext}$ and $\vec{D} = \vec{\nabla} + ie\vec{\mathcal{V}}^{\rm ext}$. Dibaryon fields in ${}^1S_0$ and ${}^3S_1$ states are denoted by $s_a$ and $t_i$, respectively, and $B_i$ is the external magnetic field given by $\vec{B} = \nabla \times \vec{\mathcal{V}}^{\rm ext}$. $\Delta_{s,t}$ are defined by the mass difference between the dibaryon and two nucleon states, i.e., $\Delta_{s,t} = m_{s,t} - 2m_N$.

LECs $y_s$ and $y_t$ represent the strength of the coupling between a two-nucleon state and a dibaryon field. They are determined from the empirical values of effective range parameters, $y_s = \frac{2}{m_N}\sqrt{\frac{2\pi}{r_0}}$ and $y_t = \frac{2}{m_N}\sqrt{\frac{2\pi}{\rho_d}}$. LECs $L_1$ and $L_2$ can be determined from the $np$ capture cross section at threshold and the deuteron magnetic moment, respectively [30].

### B. Parity-violating part

It was shown that the insertion of a nucleon loop in the propagator of a dibaryon field leaves the order of the diagram the same as that of a single dibaryon propagator [33]. As a result, PC diagrams have only dibaryon-*NN* (*dNN*) vertices for the strong interaction, and other types of strong vertices, e.g., four-nucleon contact terms belong to subleading contributions. If we are to consider the weak effects, we have to include PV interactions in a diagram. This can be easily achieved by simply replacing one PC vertex in a diagram for PC transition with a PV interaction. Even with this replacement, the remaining part of the diagram is unchanged, and so the ordering of the diagram is not affected by the insertion of a PV vertex. Therefore, it may suffice to represent the weak interactions in terms of only PV *dNN* vertices.

At low energies, two-nucleon systems are dominantly occupied by $S$-wave states, i.e., $^1S_0$ and $^3S_1$. PV interactions change the spatial parity of the $S$-wave states to the next low lying opposite parity states such as $^3P_J$ or $^1P_1$. $^1P_1$ is isosinglet, and thus it is allowed to $np$ system only. On the other hand, $^3P_J$ $(J = 0, 1)$ are isotriplet, and thus $nn$ and $pp$ as well as $np$ can occupy the states. If we consider the change of the states from $S$ wave to $P$ wave by the PV interaction, we have the following selections: $^1S_0$ to $^3P_0$ $(nn, pp, np)$, $^3S_1$ to $^1P_1$ $(np)$, and $^3S_1$ to $^3P_1$ $(np)$. As a result, we have five terms for the PV $dNN$ interactions as

$$\mathcal{L}^0_{\rm PV} = \sum_{a=1}^{3} \frac{h_d^{0sa}}{2\sqrt{2}\,\rho_d\, r_0\, m_N^{5/2}} s_a^\dagger\, N^T \sigma_2\sigma_i\tau_2\tau_a \frac{i}{2}(\overleftarrow{\nabla} - \overrightarrow{\nabla})_i N + {\rm H.c.} \tag{7}$$

$$+ \frac{h_d^{0t}}{2\sqrt{2}\rho_d\, m_N^{5/2}} t_i^\dagger\, N^T\sigma_2\tau_2 \frac{i}{2}(\overleftarrow{\nabla} - \overrightarrow{\nabla})_i N + {\rm H.c.}, \tag{8}$$

$$\mathcal{L}^1_{\rm PV} = i\frac{h_d^1}{2\sqrt{2}\rho_d\, m_N^{5/2}} \epsilon_{ijk}\, t_i^\dagger\, N^T\sigma_2\sigma_j\tau_2\tau_3 \frac{i}{2}(\overleftarrow{\nabla} - \overrightarrow{\nabla})_k N + {\rm H.c.} \tag{9}$$

The superscript in $\mathcal{L}_{\rm PV}$ denotes the change in the isospin accompanied in the interaction. In Eq. (7), $a = 1$ and 2 give isospin operator proportional to $\tau_3$ and identity matrix, respectively. With the isodoublet of the proton and the neutron, these matrices give a mixture of $nn$ and $pp$ states. These terms are irrelevant in this work, and the term corresponding to $a = 3$ generates isotriplet state of the $np$ system. Thus, we disregard the constants $h_d^{0s1}$ and $h_d^{0s2}$, and replace $h_d^{0s3}$ with $h_d^{0s}$ for brevity. Consequently we have three unknown LECs $h_d^{0s}$, $h_d^{0t}$ and $h_d^1$ for the coupling constants of PV interactions.

## III. AMPLITUDE

With the counting rules, we can arrange the pertinent Feynman diagrams order by order. We have verified in former works that applications to the PC processes were successful [29–32] already up to NLO. PC amplitude of $d\gamma \to np$ reaction is written as [29]

$$\begin{aligned} A_{\rm PC} = {} & \chi_1^\dagger \vec\sigma\sigma_2\tau_2\chi_2^{T\dagger} \cdot \{[\vec\epsilon_{(d)} \times (\hat k \times \vec\epsilon_{(\gamma)})]X_{MS} \\ & + \vec\epsilon_{(d)}\vec\epsilon_{(\gamma)}\cdot\hat p\, Y_E\} + \chi_1^\dagger\sigma_2\tau_3\tau_2\chi_2^{T\dagger} i\vec\epsilon_{(d)} \\ & \cdot(\hat k \times \vec\epsilon_{(\gamma)})\, X_{MV} + \chi_1^\dagger\vec\sigma\sigma_2\tau_3\tau_2\chi_2^{T\dagger}\cdot\{\vec\epsilon_{(d)}\vec\epsilon_{(\gamma)}\cdot\hat p\, X_E \\ & + [\vec\epsilon_{(d)}\times(\hat k\times\vec\epsilon_{(\gamma)})]\, Y_{MV}\} \\ & + \chi_1^\dagger\sigma_2\tau_2\chi_2^{T\dagger}\, i\vec\epsilon_{(d)}\cdot(\hat k\times\vec\epsilon_{(\gamma)})\, Y_{MS}, \end{aligned} \tag{10}$$

where $\vec\epsilon_{(d)}$ and $\vec\epsilon_{(\gamma)}$ are the spin polarization vectors for the incoming deuteron and photon, respectively, while $\chi_1^\dagger$ and $\chi_2^\dagger$ are the spinors of the outgoing nucleons. $\vec k$ is the momentum of an incoming photon, $\vec p$ is the relative three-momentum of the two nucleons in the final state, and unit vectors $\hat k \equiv \vec k/|\vec k|$ and $\hat p \equiv \vec p/|\vec p|$. Details for $X$'s and $Y$'s can be found in Appendix 1.

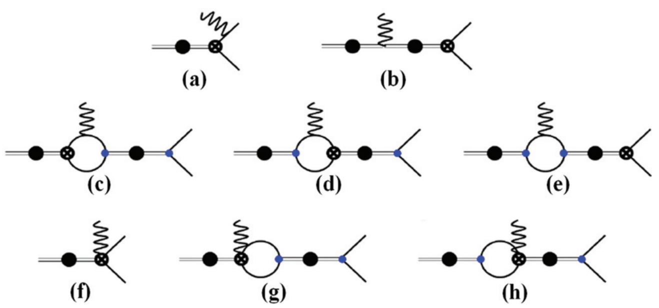


FIG. 1. (Color online) PV diagrams for $d\gamma \to \vec n p$. Single solid line denotes a nucleon, a wavy line refers to a photon, and a double line with a filled circle represents a dressed dibaryon propagator. A circle with a cross represents a PV $dNN$ vertex.

PV vertices have a spatial derivative as shown in Eqs. (7)–(9), and thus they are linear in momentum. It is natural to count the order of a PV vertex as $Q^1$. When a photon is minimally coupled to a PV vertex, it is equivalent to replacing the derivative by a photon field, and thus the order of minimally coupled PV vertices becomes $Q^0$. With the additional counting rules for the PV vertices, the diagrams for $d\gamma \to \vec n p$ are obtained and depicted in Fig. 1. If we neglect the orders of the propagators for incoming dibaryon and outgoing nucleons, the diagrams are of $Q^0$. PV amplitudes obtained from the diagrams can be written as

$$A_{\rm PV} = \sum_{i=a}^{h} A_{\rm PV}(i). \tag{11}$$

Detailed expressions for $A_{\rm PV}(i)$ are summarized in Appendix 2. The sum of both PC and PV contributions is

$$A = A_{\rm PC} + A_{\rm PV}. \tag{12}$$

The polarization is defined as

$$P_i \equiv \frac{\sigma_{i+} - \sigma_{i-}}{\sigma_{i+} + \sigma_{i-}}, \tag{13}$$

where $\sigma_{i+}$ and $\sigma_{i-}$ are the differential cross sections with the neutron spin up and down along a specific direction $i$, respectively. Polarization of neutrons can be expressed by introducing the projection operator

$$P_\pm = \tfrac{1}{2}(1-\tau_3)\tfrac{1}{2}(1 \pm \vec\sigma\cdot\hat n), \tag{14}$$

where $\hat n$ denotes the direction of the neutron spin. Squaring the amplitude given by Eq. (12) with the polarized neutrons, we obtain

$$\begin{aligned} S^{-1}\sum_{\rm spin}^{P} |A|^2 = {} & 4(|X_{MS}|^2 + |Y_{MV}|^2 - 2Y_{MV}{\rm Re}X_{MS}) \\ & + 2(|X_{MV}|^2 + |Y_{MS}|^2 - 2Y_{MS}{\rm Re}X_{MV}) \\ & + 3[1 - (\hat k\cdot\hat p)^2](|X_E|^2 + |Y_E|^2 - 2X_EY_E) \\ & \mp 2\hat n\cdot(\hat k\times\hat p)(X_E - Y_E){\rm Im}X_{MV} \\ & \mp 2(\hat k\cdot\hat n){\rm Im}\tilde f_1 \mp 2(\hat p\cdot\hat k)(\hat k\cdot\hat n){\rm Im}\tilde f_2 \\ & \mp 2(\hat p\cdot\hat n){\rm Im}\tilde f_3 \mp 2(\hat p\cdot\hat k)(\hat p\cdot\hat n){\rm Im}\tilde f_4, \end{aligned} \tag{15}$$

where $S$ is a symmetry factor for spin average, $S = 2$, and $\tilde{f}_i$'s are the PV-PC interference terms, whose details can be found in Appendix 3.

Conventions for the coordinate systems are quoted from [24]. We have the incoming photons along $\hat{k} = (0, 0, 1)$, relative momentum of the nucleons along $\hat{p} = (\sin\theta\cos\phi, \sin\theta\sin\phi, \cos\theta)$, and orthogonal basis vectors are defined as $\hat{x}' = (\cos\theta\cos\phi, \cos\theta\sin\phi, -\sin\theta)$, $\hat{y}' = (-\sin\phi, \cos\phi, 0)$, and $\hat{z}' = (\sin\theta\cos\phi, \sin\theta\sin\phi, \cos\theta)$. If the neutron spin component along $\hat{y}'$ is measured, scalar products of the unit vectors for the PV-PC interference terms $\tilde{f}_i$ vanish. In this case, we obtain the PC polarization $P_{y'}$ [29]. If one measures polarization of the neutrons along $\hat{n} = \hat{x}'$, $\hat{k}\cdot\hat{x}' = -\sin\theta$ while $\hat{p}\cdot\hat{x}' = 0$, and thus $\tilde{f}_1$ and $\tilde{f}_2$ terms are nonvanishing. With $\hat{n} = \hat{z}'$, all the $\tilde{f}_i$ terms contribute to the polarization $P_{z'}$. With $\hat{n} = \hat{x}'$ and $\hat{z}'$, one can easily check that PC interference term proportional to $\hat{n}\cdot(\hat{k}\times\hat{p})$ becomes null. Consequently, we can obtain hadronic weak effects by calculating the polarizations $P_{z'}$ and $P_{x'}$.

## IV. RESULT AND DISCUSSION

### A. Polarization along $\hat{z}'$

In this section, we present and discuss the results for $P_{z'}$. With Eqs. (13) and (15), we obtain $P_{z'}$ as

$$P_{z'} = (-2)\mathrm{Im}[(\tilde{f}_1 + \tilde{f}_4)\cos\theta + \tilde{f}_2\cos^2\theta + \tilde{f}_3]/\Sigma_{\mathrm{PC}}, \quad (16)$$

where

$$\begin{aligned}\Sigma_{\mathrm{PC}} \equiv\ & 4(|X_{MS}|^2 + |Y_{MV}|^2 - 2Y_{MV}\mathrm{Re}X_{MS}) \\ & + 2(|X_{MV}|^2 + |Y_{MS}|^2 - 2Y_{MS}\mathrm{Re}X_{MV}) \\ & + 3(1-\cos^2\theta)(|X_E|^2 + |Y_E|^2 - 2X_E Y_E). \quad (17)\end{aligned}$$

Since $\tilde{f}_i$'s contain linear combinations of $h_d^T$'s ($T = 0t$, $0s$, $1$) whose values are not known, we may rewrite the polarization in the form

$$P_{z'} \equiv c_z^{0t}h_d^{0t} + c_z^{0s}h_d^{0s} + c_z^1 h_d^1. \quad (18)$$

Coefficients $c_z^T$ are functions of the colatitude angle $\theta$ and the relative momentum $p$ (or equivalently photon energy in the laboratory frame $E_\gamma^{\mathrm{lab}}$), and they take into account the characteristics of PV as well as PC interactions of the theory. Explicit forms of $c_z^T$ can be found in Appendix 4.

In Fig. 2, we plot the numerical results for $c_z^T$'s as functions of photon energies in the laboratory frame. Angle dependences are examined by choosing three angles, $\theta_{\mathrm{lab}} = 30^\circ$, $60^\circ$, and $90^\circ$. A common feature in $c_z^T$ is that there is a minimum in the range $E_\gamma^{\mathrm{lab}} = 2.4 \sim 2.8$ MeV regardless of angles and the isospin structure of the PV vertex, i.e., the superscript $T$ in $h_d^T$. This pronounced minimum comes from the manifestation of a large scattering length $a_0$ in $^1S_0$ channel of $np$ scattering, which is embedded in the dibaryon field through the propagator of $d_s'$ of Eq. (A17). At higher energies, $c_z^{0t}$ tends to converge to a value, while $c_z^{0s}$ and $c_z^1$ show a more or less linear increase. Another noticeable behavior at higher energies is that $c_z^{0s}$ and $c_z^1$ show distinct dependence on the angles, but $c_z^{0t}$ is relatively independent of the angles, and the magnitude of the coefficients $c_z^{0t}$ and $c_z^1$ can be greater than that of $c_z^{0s}$ nearly by an order.

Next, we investigate the behavior of $c_z^T$'s by changing the angle $\theta$ continuously for a few values of $E_\gamma^{\mathrm{lab}}$ between threshold and 10 MeV. We have calculated $c_z^T$ at nine energies from $E_\gamma^{\mathrm{lab}} = 2.3$ MeV to 10 MeV, but here we only show a few results at $E_\gamma^{\mathrm{lab}} = 2.75$ and 10 MeV, because the tendency of results look more or less similar. $E_\gamma^{\mathrm{lab}} = 2.75$ MeV is chosen arbitrarily in the range $E_\gamma^{\mathrm{lab}} = 2.4 \sim 2.8$ MeV where there are minima of $c_z^T$'s. We find that the behavior of $c_z^T$ at $E_\gamma^{\mathrm{lab}} = 10$ MeV shows very unique features. Figure 3 shows $c_z^T$'s at two energies, $E_\gamma^{\mathrm{lab}} = 2.75$ MeV and 10 MeV. Figure 3(a) shows $c_z^{0s}$ is almost zero regardless of the angles. The magnitude of $c_z^{0s}$ and $c_z^{0t}$ does not exceed $7.5\times10^{-3}$, and thus the contribution from $c_z^1$ dominates at forward or backward angles, where its magnitude is greater than $2\times10^{-2}$. Figure 3(b) shows that $c_z^{0t}$ for $E_\gamma^{\mathrm{lab}} = 10$ MeV is smaller than that for 2.75 MeV, and $c_z^1$ is, though the sign is reversed, similar in behavior and in the order of magnitude. A remarkable feature is that the signs of $c_z^{0s}$ and $c_z^1$ are the same at forward angles, but opposite in backward angles. We may be able to neglect the contribution from $c_z^{0t}$ at all angles for $E_\gamma^{\mathrm{lab}} = 10$ MeV. If precise measurements of $P_{z'}$ can be performed at the energies close to threshold, we may be able to determine $h_d^1$ with less uncertainty

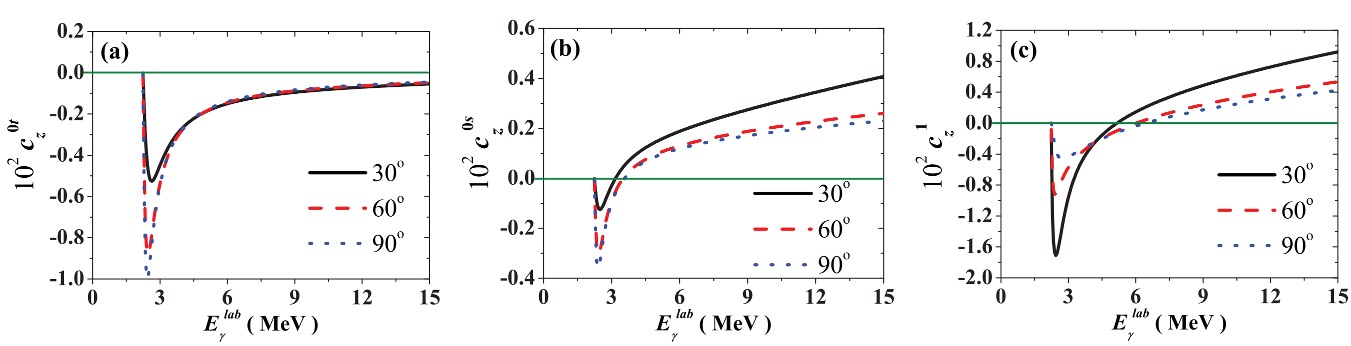


FIG. 2. (Color online) (a) $c_z^{0t}$, (b) $c_z^{0s}$, and (c) $c_z^1$ as functions of $E_\gamma^{\mathrm{lab}}$ at $\theta_{\mathrm{lab}} = 30^\circ$, $60^\circ$, and $90^\circ$.

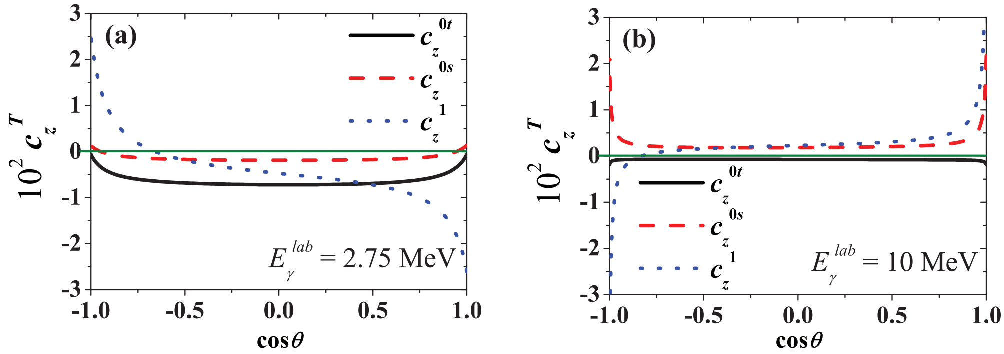

FIG. 3. (Color online) $c_z^{0t}$, $c_z^{0s}$, and $c_z^1$ as functions of $\cos\theta$ for (a) $E_\gamma^{\rm lab} = 2.75$ and (b) $E_\gamma^{\rm lab} = 10$ MeV.

since $P_{z'}$ is dominated by $c_z^1 h_d^1$ term. Next, if we can have reliable measurements at the energies around 10 MeV, we can extract the value of $h_d^{0s}$ by using the value of $h_d^1$ determined from the measurements at low energies.

Since the values of $h_d^T$ are unknown, it is not feasible to estimate directly the order of magnitude of $P_{z'}$. However, we can roughly estimate the order of magnitude of $P_{z'}$ in comparison with other PV observables.

In Ref. [18], PV up-down asymmetry of $\gamma$ rays with respect to the neutron spin direction in $\vec{n}p \to d\gamma$, $A_\gamma$ defined from

$$\frac{1}{\Gamma}\frac{d\Gamma}{\cos\theta} = 1 + A_\gamma \cos\theta, \qquad (19)$$

where $\Gamma$ is the width for $np \to d\gamma$ and $\theta$ is the angle between the photon momentum and the neutron polarization was calculated at threshold with the dibaryon fields. The result is

$$A_\gamma = -\frac{m_N^{3/2}}{2\sqrt{2\pi}} h_{33}^{(1)} \frac{1-\gamma\, a_1/3}{\kappa_1(1-\gamma\, a_0) - \gamma^2 a_0\, L_1/2}, \qquad (20)$$

where $h_{33}^{(1)}$ is the convention used for the PV $dNN$ LEC in Ref. [18]. $h_{33}^{(1)}$ and $h_d^1$ are related through

$$h_{33}^{(1)} = \frac{h_d^1}{\rho_d^{1/2} m_N^2}, \qquad (21)$$

which allows us to write $A_\gamma$ in terms of $h_d^1$ as

$$A_\gamma = -3.2 \times 10^{-3} h_d^1. \qquad (22)$$

The experimental value of $A_\gamma$ measured with cold neutrons is $-(1.5 \pm 4.8) \times 10^{-8}$ [34], and NPDGamma collaboration aims at determining the value unambiguously at the order of $10^{-8}$. The magnitude of $P_{z'}$, e.g., for $E_\gamma^{\rm lab} = 2.75$ MeV at forward angles can be larger than that of $A_\gamma$ at threshold by a factor of about 8. It seems certain that $P_{z'}$ is an observable experimentally advantageous in measurement to determine PV LEC $h_d^1$ with a better accuracy than one can achieve with $A_\gamma$.

### B. Polarization along $\hat{x}'$

Polarization along the $x'$ axis is obtained as

$$P_{x'} = 2\sin\theta\, {\rm Im}[\tilde{f}_1 + \tilde{f}_2\cos\theta]/\Sigma_{\rm PC}. \qquad (23)$$

We can cast it in the form

$$P_{x'} \equiv c_x^{0t} h_d^{0t} + c_x^{0s} h_d^{0s} + c_x^1 h_d^1, \qquad (24)$$

and investigate the characteristics of $c_x^T$'s. Complete expressions for $c_x^T$ are shown in Appendix 4.

Figure 4 shows the energy dependence of $c_x^T$'s at the angles $\theta_{\rm lab} = 30^\circ$, $60^\circ$, and $90^\circ$. $c_x^{0t}$ and $c_x^{0s}$ show the behavior and order of magnitudes similar to those of $c_z^{0t}$ and $c_z^{0s}$, respectively. The magnitude of $c_x^1$ is smaller than $c_z^1$ by roughly a factor of 2, and shows a structure with a maximum and a minimum slightly below and above 3 MeV, respectively. As was observed for $c_z^T$'s, $c_x^T$'s have extrema for $E_\gamma^{\rm lab} = 2.3 \sim 2.7$ MeV reflecting the large scattering length $a_0$ in $^1S_0$ channel.

In Fig. 5, we plot $c_x^T$ with respect to $\cos\theta$ only for $E_\gamma^{\rm lab} = 2.3$ and 2.75 MeV, though calculations of $c_x^T$ are done for various

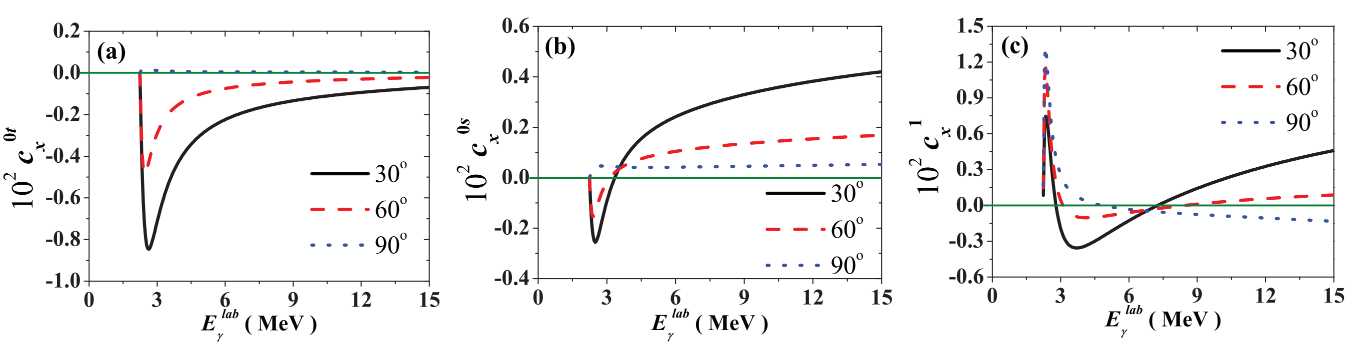

FIG. 4. (Color online) (a) $c_x^{0t}$, (b) $c_x^{0s}$, and (c) $c_x^1$ as functions of $E_\gamma^{\rm lab}$ at $\theta_{\rm lab} = 30^\circ$, $60^\circ$, and $90^\circ$.

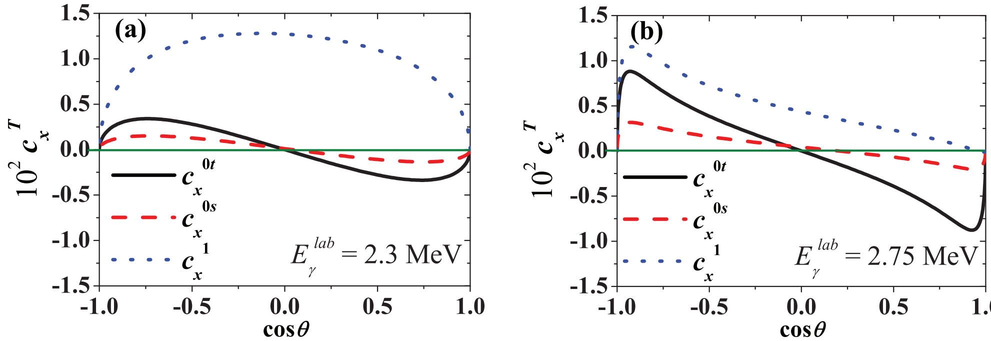


FIG. 5. (Color online) $c_x^{0t}$, $c_x^{0s}$, and $c_x^1$ as functions of $\cos\theta$ for (a) $E_\gamma^{\rm lab} = 2.3$ and (b) $E_\gamma^{\rm lab} = 2.75$ MeV.

energies of $E_\gamma^{\rm lab}$, to see the dependence of $c_x^T$ on the energy from threshold to 10 MeV. As we see from $c_z^T$'s at 10 MeV, $c_x^T$'s around 10 MeV show behaviors different from those at lower energies. However we have obtained more interesting differences among the low-energy results which are worthy of discussions. Figure 5(a) shows $c_x^T$'s for $E_\gamma^{\rm lab} = 2.3$ MeV. At $\theta = 90^\circ$, $c_x^{0t}$ and $c_x^{0s}$ are of the order of $10^{-4}$ or less, while $c_x^1 \simeq 1.3 \times 10^{-2}$. At this angle, we can neglect the contributions from $c_x^{0t}$ and $c_x^{0s}$. Again we have a unique chance to determine $h_d^1$ with a small uncertainty. Note that the magnitude of this value is roughly four times larger than the magnitude of the coefficients of $A_\gamma$ at threshold, $A_\gamma \simeq -3.2 \times 10^{-3} h_d^1$. With the measurements of $A_\gamma$ in $\vec{n}p \to d\gamma$, $P_{z'}$ at forward or backward angles, and $P_{x'}$ at around $\theta = 90^\circ$, we can simultaneously check the consistency of the theory and determine the value of $h_d^1$. In Fig. 5(b), we show the values of $c_x^T$ for $E_\gamma^{\rm lab} = 2.75$ MeV. $c_x^{0t}$ becomes maximum at $\theta \simeq 22^\circ$ with the value $c_x^{0t} \simeq -8.8 \times 10^{-3}$. The values of $c_x^{0s}$ and $c_x^1$ at this angle are $-2.0 \times 10^{-3}$ and $2.0 \times 10^{-4}$, respectively, and thus the contribution from $h_d^1$ can be safely ruled out at this angle. In Ref. [22], we calculated PV polarization $P_\gamma$ in $np \to d\gamma$ at threshold with the same theory as in the present work, where we obtained the result

$$P_\gamma = -\left(2.59 h_d^{0t} - 1.01 h_d^{0s}\right) \times 10^{-2}. \quad (25)$$

The coefficient of $h_d^{0t}$ in $P_\gamma$ is larger than $c_x^{0t}$ in $P_{x'}$ at $\theta \simeq 22^\circ$ by a factor of 3, but they are roughly similar in order. Therefore, the measurement of $P_{x'}$ at the $\theta \simeq 22^\circ$, in addition to PV $P_\gamma$ in $np \to d\gamma$, can provide a complementary constraints to determine $h_d^{0t}$ and $h_d^{0s}$. At the angles around $\theta = 157^\circ$, all the $c_x^T$'s become maximum with $c_x^1 \simeq 1.15 \times 10^{-2}$, and the ratios of $c_x^{0t}$ and $c_x^{0s}$ to $c_x^1$ are 0.76 and 0.27, respectively. By determining $h_d^{0t}$ from $P_{x'}$ at $\theta \simeq 22^\circ$, and $h_d^1$ from $A_\gamma$, $P_{z'}$ at $\theta \simeq 0^\circ$ or $180^\circ$, and $P_{x'}$ at $\theta \simeq 90^\circ$, we may be able to pin down the value of $h_d^{0s}$ through the measurement of $P_{x'}$ at the angles in the backward direction. The result will serve a countercheck of the value extracted from the measurement of $P_{z'}$ at around 10 MeV.

## V. SUMMARY

We have considered the polarization of the neutron in $d\gamma \to \vec{n}p$ with a pionless EFT incorporating dibaryon fields. Polarization along the azimuthal direction $y'$ gives us the information about the interactions that conserve parity. Along the radial ($z'$) and colatitude ($x'$) directions, on the other hand, nonvanishing contributions reflect the effect of PV interactions. We focused on the PV components of the polarization, and calculated $P_{z'}$ and $P_{x'}$ as functions of the incident photon energies up to 15 MeV. Since the coefficients $c_z^T$'s and $c_x^T$'s can be evaluated at different angles and energies, one can determine the unknown PV LECs by comparing the calculated $P_{z'}$ and $P_{x'}$ with the experimental values.

At low energies, pionless EFT with dibaryon fields is verified to a good accuracy for many observables in the two-nucleon processes, but care should be taken as we increase energy near ~15 MeV [35]. Therefore, if measurement is performed, it may be most desirable to have it done at low energies.

By choosing the photon energy as 2.75 MeV, we explored the dependence of $c_z^T$ and $c_x^T$ on the angle $\theta$. Concerning $P_{z'}$, the coefficients of the isoscalar components of the PV interaction, $c_z^{0s}$ and $c_z^{0t}$, are more or less constant in the angle, but the coefficient of the isovector component, $c_z^1$, changes drastically in the forward and backward angles. In these directions, $P_{z'}$ is exclusively dominated by the PV isovector interaction, and thus the measurement of $P_{z'}$ along with $A_\gamma$ in $\vec{n}p \to d\gamma$ can provide a chance for a unique determination of $h_d^1$. $P_{x'}$ is expected to give more information about the PV LECs. At the angles close to the forward direction, the values of $c_x^{0t}$ are more significant than those of $c_x^{0s}$ and $c_x^1$, and thus $P_{x'}$ is expected to be dominated by $h_d^{0t}$. On the other hand, in the backward directions, contributions from $h_d^1$, $h_d^{0t}$, and $h_d^{0s}$ terms are expected to be of the same order. By combining the measurements of $P_{z'}$ and $P_{x'}$ at various angles, we can determine the PV LECs in the $np$ system, $h_d^{0t}$, $h_d^{0s}$, and $h_d^1$.

The fact that the value of $P_{z'}$ can be an order of magnitude larger than that of $A_\gamma$ is a striking result. Since the prediction can imply significant impact on the experiments, the results in this work need to be counterchecked by other calculations. One possibility is to adopt the DDH potential, and obtain the results for $P_{z'}$ and $P_{x'}$ in terms of the PV meson-nucleon coupling constants. Many PV observables in the two-nucleon systems were already calculated in terms of the DDH potential. The work is in progress for evaluating $P_{z'}$ and $P_{x'}$ [36].

## ACKNOWLEDGMENTS

The work of C.H.H. and S.I.A. is supported by the Basic Science Research Program through the National Research Foundation of Korea (NRF) funded by the Ministry of Education, Science and Technology Grant No. 2010-0023661, the work of J.W.S. by Basic Science Research Program through the NRF funded by the Ministry of Education, Science and Technology Grant No. 2011-0025116, and the work of S.W.H. by Basic Science Research Program through the NRF funded by the Ministry of Education, Science and Technology Grant No. 2012R1A1A2007826.


## APPENDIX: SUMMARY OF LENGTHY EXPRESSIONS

### 1. PC terms

Several quantities in the PC amplitude up to NLO in Eq. (10) are expressed as follows.

$$X_{MV} = -\sqrt{\frac{\pi\gamma}{1-\gamma\rho_d}}\frac{1}{\frac{1}{a_0}+ip-\frac{1}{2}r_0p^2}\frac{1}{2m_N}\left\{\mu_V\left[\arccos\left(\frac{m_N}{\sqrt{\left(m_N+\frac{1}{2}\omega_\gamma\right)^2-p^2}}\right)+i\ln\left(\frac{m_N+\frac{1}{2}\omega_\gamma+p}{\sqrt{\left(m_N+\frac{1}{2}\omega_\gamma\right)^2-p^2}}\right)\right]\right.$$
$$\left.-\frac{\mu_V}{m_N}\left(\frac{1}{a_0}+ip-\frac{1}{2}r_0p^2\right)F^+ +\omega_\gamma L_1\right\}, \tag{A1}$$

$$X_{MS} = -\sqrt{\frac{\pi\gamma}{1-\gamma\rho_d}}\frac{1}{\gamma+ip-\frac{1}{2}\rho_d(\gamma^2+p^2)}\frac{1}{2m_N}\left\{\mu_S\left[\arccos\left(\frac{m_N}{\sqrt{\left(m_N+\frac{1}{2}\omega_\gamma\right)^2-p^2}}\right)+i\ln\left(\frac{m_N+\frac{1}{2}\omega_\gamma+p}{\sqrt{\left(m_N+\frac{1}{2}\omega_\gamma\right)^2-p^2}}\right)\right]\right.$$
$$\left.-\frac{\mu_S}{m_N}\left[\gamma+ip-\frac{1}{2}\rho_d(\gamma^2+p^2)\right]F^+ +2\omega_\gamma L_2\right\}, \tag{A2}$$

$$X_E = \sqrt{\frac{\pi\gamma}{1-\gamma\rho_d}}\frac{1}{m_N^2}\frac{p}{\omega_\gamma}F^+,\quad Y_E = \sqrt{\frac{\pi\gamma}{1-\gamma\rho_d}}\frac{1}{m_N^2}\frac{p}{\omega_\gamma}F^-, \tag{A3}$$

$$Y_{MV} = \sqrt{\frac{\pi\gamma}{1-\gamma\rho_d}}\frac{\mu_V}{2m_N^2}F^-,\quad Y_{MS} = \sqrt{\frac{\pi\gamma}{1-\gamma\rho_d}}\frac{\mu_S}{2m_N^2}F^-, \tag{A4}$$

where $\omega_\gamma$ is the incident photon energy in the c.m. frame, and

$$F^\pm = \frac{1}{2}\left[\frac{1}{1+\frac{\omega_\gamma}{2m_N}-\frac{\vec{p}\cdot\hat{k}}{m_N}} \pm \frac{1}{1+\frac{\omega_\gamma}{2m_N}+\frac{\vec{p}\cdot\hat{k}}{m_N}}\right]. \tag{A5}$$

### 2. PV amplitudes

Each amplitude for diagrams from Fig. 1(a) to Fig. 1(h) can be expressed as follows. $\chi_1^\dagger$ and $\chi_2^{T\dagger}$ are the spinors of the nucleons in the final state.

$$\begin{aligned}
iA_{\rm PV}(a) = {}& Ch_d^{0t}\Big[(i)\chi_1^\dagger\sigma_2\tau_2\chi_2^{T\dagger}\epsilon_{(d)i}\epsilon_{(\gamma)j}\hat{k}_i\hat{p}_j\frac{p}{m_N}F^+ - (i)\chi_1^\dagger\sigma_2\tau_2\chi_2^{T\dagger}\epsilon_{(d)i}\epsilon_{(\gamma)j}\hat{p}_i\hat{p}_j\frac{2p^2}{m_N\omega_\gamma}F^- \\
&+(i)\chi_1^\dagger\sigma_2\tau_3\tau_2\chi_2^{T\dagger}\epsilon_{(d)i}\epsilon_{(\gamma)j}\hat{k}_i\hat{p}_j\frac{p}{m_N}F^- - (i)\chi_1^\dagger\sigma_2\tau_3\tau_2\chi_2^{T\dagger}\epsilon_{(d)i}\epsilon_{(\gamma)j}\hat{p}_i\hat{p}_j\frac{2p^2}{m_N\omega_\gamma}F^+ \\
&+\chi_1^\dagger\sigma_i\sigma_2\tau_2\chi_2^{T\dagger}\epsilon_{ijk}\epsilon_{(d)a}\epsilon_{(\gamma)k}\hat{k}_j\hat{p}_a\frac{\mu_S}{m_N}pF^- - \chi_1^\dagger\sigma_i\sigma_2\tau_2\chi_2^{T\dagger}\epsilon_{ijk}\epsilon_{(d)a}\epsilon_{(\gamma)k}\hat{k}_j\hat{k}_a\frac{\mu_S}{2m_N}\omega_\gamma F^+ \\
&+\chi_1^\dagger\sigma_i\sigma_2\tau_3\tau_2\chi_2^{T\dagger}\epsilon_{ijk}\epsilon_{(d)a}\epsilon_{(\gamma)k}\hat{k}_j\hat{p}_a\frac{\mu_V}{m_N}pF^+ - \chi_1^\dagger\sigma_i\sigma_2\tau_3\tau_2\chi_2^{T\dagger}\epsilon_{ijk}\epsilon_{(d)a}\epsilon_{(\gamma)k}\hat{k}_j\hat{k}_a\frac{\mu_V}{2m_N}\omega_\gamma F^-\Big] \\
&+Ch_d^1\Big[\chi_1^\dagger\sigma_i\sigma_2\tau_2\chi_2^{T\dagger}\epsilon_{ijk}\epsilon_{(d)j}\epsilon_{(\gamma)a}\hat{p}_k\hat{p}_a\frac{2p^2}{m_N\omega_\gamma}F^+ - \chi_1^\dagger\sigma_i\sigma_2\tau_2\chi_2^{T\dagger}\epsilon_{ijk}\epsilon_{(d)j}\epsilon_{(\gamma)a}\hat{k}_k\hat{p}_a\frac{p}{m_N}F^- \\
&+\chi_1^\dagger\sigma_i\sigma_2\tau_3\tau_2\chi_2^{T\dagger}\epsilon_{ijk}\epsilon_{(d)j}\epsilon_{(\gamma)a}\hat{p}_k\hat{p}_a\frac{2p^2}{m_N\omega_\gamma}F^- - \chi_1^\dagger\sigma_i\sigma_2\tau_3\tau_2\chi_2^{T\dagger}\epsilon_{ijk}\epsilon_{(d)j}\epsilon_{(\gamma)a}\hat{k}_k\hat{p}_a\frac{p}{m_N}F^+ \\
&+(i)\chi_1^\dagger\sigma_2\tau_2\chi_2^{T\dagger}\epsilon_{(d)i}\epsilon_{(\gamma)i}\left(\frac{\mu_V}{2m_N}\omega_\gamma F^- - \hat{p}_j\hat{k}_j\frac{\mu_V}{m_N}pF^-\right) + (i)\chi_1^\dagger\sigma_2\tau_2\chi_2^{T\dagger}\epsilon_{(d)i}\epsilon_{(\gamma)j}\hat{k}_i\hat{p}_j\frac{\mu_V}{m_N}pF^+
\end{aligned}$$

$$+ \chi_1^\dagger \sigma_i \sigma_2 \tau_2 \chi_2^{T\dagger} \epsilon_{abc} \epsilon_{(d)c} \epsilon_{(\gamma)i} \hat{k}_a \hat{p}_b \frac{\mu_V}{m_N} p F^- - \chi_1^\dagger \sigma_i \sigma_2 \tau_2 \chi_2^{T\dagger} \epsilon_{abc} \epsilon_{(d)c} \epsilon_{(\gamma)a} \hat{k}_i \hat{p}_b \frac{\mu_V}{m_N} p F^-$$
$$+ \chi_1^\dagger \sigma_i \sigma_2 \tau_2 \chi_2^{T\dagger} \epsilon_{abc} \epsilon_{(d)c} \epsilon_{(\gamma)a} \hat{k}_i \hat{k}_b \frac{\mu_V}{2m_N} \omega_\gamma F^+ + (i) \chi_1^\dagger \sigma_2 \tau_3 \tau_2 \chi_2^{T\dagger} \epsilon_{(d)i} \epsilon_{(\gamma)i} \left( \frac{\mu_S}{2m_N} \omega_\gamma F^+ - \hat{p}_j \hat{k}_j \frac{\mu_S}{m_N} p F^- \right)$$
$$+ (i) \chi_1^\dagger \sigma_2 \tau_3 \tau_2 \chi_2^{T\dagger} \epsilon_{(d)i} \epsilon_{(\gamma)j} \hat{k}_i \hat{p}_j \frac{\mu_S}{m_N} p F^- + \chi_1^\dagger \sigma_i \sigma_2 \tau_3 \tau_2 \chi_2^{T\dagger} \epsilon_{abc} \epsilon_{(d)c} \epsilon_{(\gamma)i} \hat{k}_a \hat{p}_b \frac{\mu_S}{m_N} p F^+$$
$$- \chi_1^\dagger \sigma_i \sigma_2 \tau_3 \tau_2 \chi_2^{T\dagger} \epsilon_{abc} \epsilon_{(d)c} \epsilon_{(\gamma)a} \hat{k}_i \hat{p}_b \frac{\mu_S}{m_N} p F^+ + \chi_1^\dagger \sigma_i \sigma_2 \tau_3 \tau_2 \chi_2^{T\dagger} \epsilon_{abc} \epsilon_{(d)c} \epsilon_{(\gamma)a} \hat{k}_i \hat{k}_b \frac{\mu_S}{2m_N} \omega_\gamma F^- \Bigg], \tag{A6}$$

$$i A_{\rm PV}(b) = C p\, \omega_\gamma \big[ h_d^{0s}\, d_s' L_1 \chi_1^\dagger \sigma_i \sigma_2 \tau_3 \tau_2 \chi_2^{T\dagger} \epsilon_{abc} \epsilon_{(d)a} \epsilon_{(\gamma)b} \hat{k}_c \hat{p}_i + h_d^{0t}\, d_t' (i) 2 L_2 \chi_1^\dagger \sigma_2 \tau_2 \chi_2^{T\dagger} (\epsilon_{(d)i} \epsilon_{(\gamma)i} \hat{k}_j \hat{p}_j - \epsilon_{(d)i} \epsilon_{(\gamma)j} \hat{k}_i \hat{p}_j)$$
$$+ h_d^1\, d_t' 2 L_2 \chi_1^\dagger \sigma_i \sigma_2 \tau_3 \tau_2 \chi_2^{T\dagger} (\epsilon_{ijk} \epsilon_{(d)a} \epsilon_{(\gamma)a} \hat{k}_k \hat{p}_j - \epsilon_{ijk} \epsilon_{(d)a} \epsilon_{(\gamma)k} \hat{k}_a \hat{p}_j) \big], \tag{A7}$$

$$i A_{\rm PV}(c) = C d_t' \big[ h_d^1 \chi_1^\dagger \sigma_i \sigma_2 \tau_2 \chi_2^{T\dagger} \epsilon_{abc} \epsilon_{(d)c} \epsilon_{(\gamma)a} \hat{k}_i \hat{k}_b \mu_V (m_N f_1 - \gamma - ip) - h_d^{0t} \chi_1^\dagger \sigma_i \sigma_2 \tau_2 \chi_2^{T\dagger} \epsilon_{ijk} \epsilon_{(d)a} \epsilon_{(\gamma)k} \hat{k}_j \hat{k}_a \mu_S (m_N f_1 - \gamma - ip)$$
$$- h_d^1 \chi_1^\dagger \sigma_i \sigma_2 \tau_2 \chi_2^{T\dagger} \epsilon_{ijk} \epsilon_{(d)j} \epsilon_{(\gamma)k} f_2 \big] + C d_s' \bigg[ h_d^1 (i) \chi_1^\dagger \sigma_2 \tau_3 \tau_2 \chi_2^{T\dagger} \epsilon_{(d)i} \epsilon_{(\gamma)i} \mu_S \left\{ \left( m_N + \frac{1}{2} \omega_\gamma \right) f_1 - \gamma - ip \right\}$$
$$+ h_d^{0t} (i) \chi_1^\dagger \sigma_2 \tau_3 \tau_2 \chi_2^{T\dagger} \epsilon_{(d)i} \epsilon_{(\gamma)i} f_2 \bigg], \tag{A8}$$

$$i A_{\rm PV}(d) = C d_t' \bigg[ h_d^{0t} \chi_1^\dagger \sigma_i \sigma_2 \tau_2 \chi_2^{T\dagger} \epsilon_{abc} \epsilon_{(d)c} \epsilon_{(\gamma)a} \hat{k}_i \hat{k}_b \mu_S \left\{ \left( m_N + \frac{1}{2} \omega_\gamma \right) f_1 - \gamma - ip \right\}$$
$$- h_d^1 \chi_1^\dagger \sigma_i \sigma_2 \tau_2 \chi_2^{T\dagger} \epsilon_{ijk} \epsilon_{(d)a} \epsilon_{(\gamma)k} \hat{k}_j \hat{k}_a \mu_V \left\{ \left( m_N + \frac{1}{2} \omega_\gamma \right) f_1 - \gamma - ip \right\} - h_d^1 \chi_1^\dagger \sigma_i \sigma_2 \tau_2 \chi_2^{T\dagger} \epsilon_{ijk} \epsilon_{(d)j} \epsilon_{(\gamma)k} f_2 \bigg]$$
$$+ C d_s' \bigg[ h_d^{0s} (i) \chi_1^\dagger \sigma_2 \tau_3 \tau_2 \chi_2^{T\dagger} \epsilon_{(d)i} \epsilon_{(\gamma)i} \mu_V \left\{ \left( m_N + \frac{1}{2} \omega_\gamma \right) f_1 - \gamma - ip \right\} + h_d^{0s} (i) \chi_1^\dagger \sigma_2 \tau_3 \tau_2 \chi_2^{T\dagger} \epsilon_{(d)i} \epsilon_{(\gamma)i} f_2 \bigg], \tag{A9}$$

$$i A_{\rm PV}(e) = C f_1 p \big[ h_d^{0s}\, d_s' \mu_V \chi_1^\dagger \sigma_i \sigma_2 \tau_3 \tau_2 \chi_2^{T\dagger} \epsilon_{abc} \epsilon_{(d)c} \epsilon_{(\gamma)a} \hat{k}_b \hat{p}_i + h_d^{0t}\, d_t' \mu_S (i) \chi_1^\dagger \sigma_2 \tau_2 \chi_2^{T\dagger} (\epsilon_{(d)i} \epsilon_{(\gamma)i} \hat{k}_j \hat{p}_j - \epsilon_{(d)i} \epsilon_{(\gamma)j} \hat{k}_i \hat{p}_j)$$
$$+ h_d^1\, d_t' \mu_S \chi_1^\dagger \sigma_i \sigma_2 \tau_3 \tau_2 \chi_2^{T\dagger} (\epsilon_{ijk} \epsilon_{(d)a} \epsilon_{(\gamma)a} \hat{k}_k \hat{p}_j - \epsilon_{ijk} \epsilon_{(d)a} \epsilon_{(\gamma)k} \hat{k}_a \hat{p}_j) \big], \tag{A10}$$

$$i A_{\rm PV}(f) = C \big[ h_d^{0t} (i) \chi_1^\dagger \sigma_2 \tau_3 \tau_2 \chi_2^{T\dagger} \epsilon_{(d)i} \epsilon_{(\gamma)i} - h_d^1 \chi_1^\dagger \sigma_i \sigma_2 \tau_2 \chi_2^{T\dagger} \epsilon_{ijk} \epsilon_{(d)j} \epsilon_{(\gamma)k} \big], \tag{A11}$$

$$i A_{\rm PV}(g) = C p \big[ h_d^{0t}\, d_s' \chi_1^\dagger \sigma_2 \tau_3 \tau_2 \chi_2^{T\dagger} \epsilon_{(d)i} \epsilon_{(\gamma)i} + h_d^1\, d_t' (i) \chi_1^\dagger \sigma_i \sigma_2 \tau_2 \chi_2^{T\dagger} \epsilon_{ijk} \epsilon_{(d)j} \epsilon_{(\gamma)k} \big], \tag{A12}$$

$$i A_{\rm PV}(h) = C \gamma \big[ h_d^{0s}\, d_s' (i) \chi_1^\dagger \sigma_2 \tau_3 \tau_2 \chi_2^{T\dagger} \epsilon_{(d)i} \epsilon_{(\gamma)i} - h_d^1\, d_t' \chi_1^\dagger \sigma_i \sigma_2 \tau_2 \chi_2^{T\dagger} \epsilon_{ijk} \epsilon_{(d)j} \epsilon_{(\gamma)k} \big], \tag{A13}$$

where

$$C = \frac{1}{2} \sqrt{\frac{\gamma \rho_d}{1 - \gamma \rho_d}} \frac{1}{2\sqrt{2} \rho_d m_N^{5/2}}, \tag{A14}$$

$$f_1 = \arccos \left( \frac{m_N}{\sqrt{\left(m_N + \frac{1}{2}\omega_\gamma\right)^2 - p^2}} \right) + i \ln \left( \frac{m_N + \frac{1}{2}\omega_\gamma + p}{\sqrt{\left(m_N + \frac{1}{2}\omega_\gamma\right)^2 - p^2}} \right), \tag{A15}$$

$$f_2 = \frac{1}{\omega_\gamma} \left[ m_N \gamma + i \left( m_N + \frac{1}{2} \omega_\gamma \right) p - \left\{ \left( m_N + \frac{1}{2} \omega_\gamma \right)^2 - p^2 \right\} f_1 \right], \tag{A16}$$

$$d_s' = \frac{1}{\frac{1}{a_0} + ip - \frac{1}{2} r_0 p^2}, \quad d_t' = \frac{1}{\gamma + ip - \frac{1}{2} \rho_d (\gamma^2 + p^2)}. \tag{A17}$$

### 3. PV-PC interference terms

The transition rate can be written as

$$S^{-1} \sum_{\rm spin}^{P} |A|^2 = 4(|X_{MS}|^2 + |Y_{MV}|^2 - 2 Y_{MV} {\rm Re} X_{MS}) + 2(|X_{MV}|^2 + |Y_{MS}|^2 - 2 Y_{MS} {\rm Re} X_{MV})$$
$$+ 3(1 - (\hat{k} \cdot \hat{p})^2)(|X_E|^2 + |Y_E|^2 - 2 X_E Y_E) \pm 2 \hat{n} \cdot (\hat{k} \times \hat{p})(Y_E - X_E) {\rm Im} X_{MV}$$
$$\pm i(\hat{k} \cdot \hat{n})[\tilde{f}_1 - \tilde{f}_1^*] \pm i(\hat{p} \cdot \hat{k})(\hat{k} \cdot \hat{n})[\tilde{f}_2 - \tilde{f}_2^*] \pm i(\hat{p} \cdot \hat{n})[\tilde{f}_3 - \tilde{f}_3^*] \pm i(\hat{p} \cdot \hat{k})(\hat{p} \cdot \hat{n})[\tilde{f}_4 - \tilde{f}_4^*]. \tag{A18}$$

PV-PC interference terms $\tilde{f}_i$ are given as

$$\tilde{f}_1 = \big[h_d^{0t}\tilde{Z}_{MS}^{pg} - h_d^{0s}\tilde{Z}_{MV}^{pg} + h_d^1\tilde{Z}_{MS}^{pg}\big](X_E^* - Y_E^*) - \big[2h_d^{0t}\mu_S\tilde{Z}^{tg} + h_d^1\big(\tilde{X}_{pp} - \tilde{Y}_{pp} + 2\mu_V\tilde{X}_{gg} - 2\mu_S\tilde{Y}_{gg} + 2\tilde{Z}_E^1 + 2\mu_V\tilde{Z}^t\big)\big]X_{MV}^*$$
$$+ \big[2h_d^{0t}\big(\tilde{Z}_E^{0t} + \mu_S\tilde{Z}^t\big) + 2h_d^{0s}\big(\tilde{Z}_E^{0s} + \mu_V\tilde{Z}^{sg}\big) - 2h_d^1\big(\tilde{Z}_E^1 - \mu_V\tilde{Z}^{tg} - \mu_S\tilde{Z}^s\big)\big]Y_{MV}^*$$
$$+ \big[h_d^{0t}(\tilde{X}_{pp} - \tilde{Y}_{pp} - 2\mu_S\tilde{X}_{gg} + 2\mu_V\tilde{Y}_{gg} - 2\tilde{Z}_E^{0t} - 2\mu_S\tilde{Z}^t) - 2h_d^{0s}\big(\tilde{Z}_E^{0s} + \mu_V\tilde{Z}^{sg}\big)$$
$$+ h_d^1\big(\tilde{X}_{pp} - \tilde{Y}_{pp} - 2\mu_S\tilde{X}_{gg} + 2\mu_V\tilde{Y}_{gg} + 2\tilde{Z}_E^1 - 2\mu_V\tilde{Z}^{tg} - 2\mu_S\tilde{Z}^s\big)\big]X_{MS}^* + \big[2h_d^{0t}\mu_S\tilde{Z}^{tg} + 2h_d^1\big(\tilde{Z}_E^1 + \mu_V\tilde{Z}^t\big)\big]Y_{MS}^*, \tag{A19}$$

$$\tilde{f}_2 = \big[-h_d^{0t}\big(\tilde{Z}_E^{0t} + \mu_S\tilde{Z}^t - \mu_S\tilde{Z}^{tg}\big) - h_d^{0s}\big(\tilde{Z}_E^{0s} + \mu_V\tilde{Z}^{sg}\big) + h_d^1\big(2\tilde{Z}_E^1 + \mu_V\tilde{Z}^t - \mu_S\tilde{Z}^s - \mu_V\tilde{Z}^{tg}\big)\big](X_E^* - Y_E^*)$$
$$+ \big[h_d^{0t}(\mu_V\tilde{X}_{pg} - \mu_S\tilde{Y}_{pg}) - h_d^1(\tilde{X}_{pg} - \tilde{Y}_{pg} + \mu_S\tilde{X}_{pg} - \mu_V\tilde{Y}_{pg})\big]X_{MV}^* - \big[h_d^{0t}\tilde{Z}_{MS}^{pg} - h_d^1\tilde{Z}_{MS}^{pg}\big]Y_{MV}^*$$
$$+ \big[h_d^{0t}\big(\tilde{X}_{pg} - \tilde{Y}_{pg} - \mu_V\tilde{X}_{pg} + \mu_S\tilde{Y}_{pg} + \tilde{Z}_{MS}^{pg}\big) + h_d^1\big(\tilde{X}_{pg} - \tilde{Y}_{pg} - \mu_V\tilde{X}_{pg} + \mu_S\tilde{Y}_{pg} + 2\mu_S\tilde{X}_{pg} - 2\mu_V\tilde{Y}_{pg} - \tilde{Z}_{MS}^{pg}\big)\big]X_{MS}^*, \tag{A20}$$

$$\tilde{f}_3 = \big[h_d^{0t}\big(\tilde{Z}_E^{0t} + \mu_S\tilde{Z}^t - \mu_S\tilde{Z}^{tg}\big) + h_d^{0s}\big(\tilde{Z}_E^{0s} + \mu_V\tilde{Z}^{sg}\big) - h_d^1\big(2\tilde{Z}_E^1 - \mu_V\tilde{Z}^{tg} - \mu_S\tilde{Z}^s + \mu_V\tilde{Z}^t\big)\big](X_E^* - Y_E^*)$$
$$- \big[h_d^{0t}(\mu_V\tilde{X}_{pg} - \mu_S\tilde{Y}_{pg}) - 2h_d^{0s}\tilde{Z}_{MV}^{pg} - h_d^1(\tilde{X}_{pg} - \tilde{Y}_{pg} - \mu_S\tilde{X}_{pg} + \mu_V\tilde{Y}_{pg})\big]X_{MV}^* - \big[h_d^{0t}\tilde{Z}_{MS}^{pg} + 3h_d^1\tilde{Z}_{MS}^{pg}\big]Y_{MV}^*$$
$$- \big[h_d^{0t}\big(\tilde{X}_{pg} - \tilde{Y}_{pg} + \mu_V\tilde{X}_{pg} - \mu_S\tilde{Y}_{pg} - \tilde{Z}_{MS}^{pg}\big) + h_d^1\big(\tilde{X}_{pg} - \tilde{Y}_{pg} + \mu_V\tilde{X}_{pg} - \mu_S\tilde{Y}_{pg} + 2\mu_S\tilde{X}_{pg} - 2\mu_V\tilde{Y}_{pg} - 3\tilde{Z}_{MS}^{pg}\big)\big]X_{MS}^*$$
$$- \big[2h_d^{0s}\tilde{Z}_{MV}^{pg}\big]Y_{MS}^*, \tag{A21}$$

$$\tilde{f}_4 = \big[-h_d^{0t}\tilde{Z}_{MS}^{pg} + h_d^{0s}\tilde{Z}_{MV}^{pg} - h_d^1\tilde{Z}_{MS}^{pg}\big](X_E^* - Y_E^*) + \big[h_d^1(\tilde{X}_{pp} - \tilde{Y}_{pp})\big]X_{MV}^* - \big[h_d^{0t}(\tilde{X}_{pp} - \tilde{Y}_{pp}) + h_d^1(\tilde{X}_{pp} - \tilde{Y}_{pp})\big]X_{MS}^*, \tag{A22}$$

where

$$\tilde{X}_{pg} = C\frac{1}{m_N\omega_\gamma}(p\omega_\gamma)F^+, \quad \tilde{Y}_{pg} = C\frac{1}{m_N\omega_\gamma}(p\omega_\gamma)F^-, \tag{A23}$$

$$\tilde{X}_{pp} = C\frac{1}{m_N\omega_\gamma}(2p^2)F^+, \quad \tilde{Y}_{pp} = C\frac{1}{m_N\omega_\gamma}(2p^2)F^-, \tag{A24}$$

$$\tilde{X}_{gg} = C\frac{1}{m_N\omega_\gamma}\left(\frac{\omega_\gamma{}^2}{2}\right)F^+, \quad \tilde{Y}_{gg} = C\frac{1}{m_N\omega_\gamma}\left(\frac{\omega_\gamma{}^2}{2}\right)F^-, \tag{A25}$$

$$\tilde{Z}_E^{0s} = Cd_s'[f_2 + \gamma], \quad \tilde{Z}_E^{0t} = Cd_s'\left[f_2 + \frac{1}{a_0} - \frac{1}{2}r_0p^2\right], \tag{A26}$$

$$\tilde{Z}_E^1 = -Cd_t'\left[2f_2 + 2\gamma - \frac{1}{2}\rho_d(\gamma^2 + p^2)\right], \tag{A27}$$

$$\tilde{Z}^{sg} = Cd_s'\left[\left(m_N + \frac{1}{2}\omega_\gamma\right)f_1 - \gamma - ip\right], \quad \tilde{Z}^s = Cd_s'[m_Nf_1 - \gamma - ip], \tag{A28}$$

$$\tilde{Z}^{tg} = Cd_t'\left[\left(m_N + \frac{1}{2}\omega_\gamma\right)f_1 - \gamma - ip\right], \quad \tilde{Z}^t = Cd_t'[m_Nf_1 - \gamma - ip], \tag{A29}$$

$$\tilde{Z}_{MS}^{pg} = Cd_t'p[\mu_Sf_1 + 2\omega_\gamma L_2], \quad \tilde{Z}_{MV}^{pg} = Cd_s'p[\mu_Vf_1 + \omega_\gamma L_1]. \tag{A30}$$

### 4. $c_z^T$ and $c_x^T$

$$c_z^{0t} = -\frac{2}{\Sigma_{\rm PC}}{\rm Im}\big[\sin^2\theta\big(\tilde{Z}_E^{0t} + \mu_S\tilde{Z}^t - \mu_S\tilde{Z}^{tg}\big)(X_E^* - Y_E^*) + \{-2\cos\theta\mu_S\tilde{Z}^{tg} - \sin^2\theta(\mu_V\tilde{X}_{pg} - \mu_S\tilde{Y}_{pg})\}X_{MV}^*$$
$$+ \big\{2\cos\theta\big(\tilde{Z}_E^{0t} + \mu_S\tilde{Z}^t\big) - (1 + \cos^2\theta)\tilde{Z}_{MS}^{pg}\big\}Y_{MV}^* + \big\{2\cos\theta(-\mu_S\tilde{X}_{gg} + \mu_V\tilde{Y}_{gg} - \tilde{Z}_E^{0t} - \mu_S\tilde{Z}^t) - \sin^2\theta(\tilde{X}_{pg} - \tilde{Y}_{pg})$$
$$+ (1 + \cos^2\theta)\big(-\mu_V\tilde{X}_{pg} + \mu_S\tilde{Y}_{pg} + \tilde{Z}_{MS}^{pg}\big)\big\}X_{MS}^* + 2\cos\theta\mu_S\tilde{Z}^{tg}Y_{MS}^*\big], \tag{A31}$$

$$c_z^{0s} = -\frac{2}{\Sigma_{\rm PC}}{\rm Im}\big[\sin^2\theta\big(\tilde{Z}_E^{0s} + \mu_V\tilde{Z}^{sg}\big)(X_E^* - Y_E^*) + 2\tilde{Z}_{MV}^{pg}X_{MV}^*$$
$$+ 2\cos\theta\big(\tilde{Z}_E^{0s} + \mu_V\tilde{Z}^{sg}\big)Y_{MV}^* - 2\cos\theta\big(\tilde{Z}_E^{0s} + \mu_V\tilde{Z}^{sg}\big)X_{MS}^* - 2\tilde{Z}_{MV}^{pg}Y_{MS}^*\big], \tag{A32}$$

$$c_z^1 = -\frac{2}{\Sigma_{\rm PC}}{\rm Im}\big[\sin^2\theta\big(-2\tilde{Z}_E^1 + \mu_V\tilde{Z}^{tg} + \mu_S\tilde{Z}^s - \mu_V\tilde{Z}^t\big)(X_E^* - Y_E^*) + \{-2\cos\theta(\mu_V\tilde{X}_{gg} - \mu_S\tilde{Y}_{gg} + \tilde{Z}_E^1 + \mu_V\tilde{Z}^t)$$
$$+ \sin^2\theta(\tilde{X}_{pg} - \tilde{Y}_{pg}) - (1 + \cos^2\theta)(\mu_S\tilde{X}_{pg} - \mu_V\tilde{Y}_{pg})\}X_{MV}^* + \big\{-2\cos\theta\big(\tilde{Z}_E^1 - \mu_V\tilde{Z}^{tg} - \mu_S\tilde{Z}^s\big) - (3 - \cos^2\theta)\tilde{Z}_{MS}^{pg}\big\}Y_{MV}^*$$
$$+ \big\{2\cos\theta(-\mu_S\tilde{X}_{gg} + \mu_V\tilde{Y}_{gg} + \tilde{Z}_E^1 - \mu_V\tilde{Z}^{tg} - \mu_S\tilde{Z}^s) - \sin^2\theta(\tilde{X}_{pg} - \tilde{Y}_{pg})$$
$$- (1 + \cos^2\theta)(\mu_V\tilde{X}_{pg} - \mu_S\tilde{Y}_{pg}) - 2\sin^2\theta(\mu_S\tilde{X}_{pg} - \mu_V\tilde{Y}_{pg}) + (3 - \cos^2\theta)\tilde{Z}_{MS}^{pg}\big\}X_{MS}^* + 2\cos\theta\big(\tilde{Z}_E^1 + \mu_V\tilde{Z}^t\big)Y_{MS}^*\big], \tag{A33}$$

$$c_x^{0t} = \frac{2}{\Sigma_{\rm PC}}\sin\theta{\rm Im}\big[\big\{\tilde{Z}_{MS}^{pg} - \cos\theta\big(\tilde{Z}_E^{0t} + \mu_S\tilde{Z}^t - \mu_S\tilde{Z}^{tg}\big)\big\}(X_E^* - Y_E^*) + \{-2\mu_S\tilde{Z}^{tg} + \cos\theta(\mu_V\tilde{X}_{pg} - \mu_S\tilde{Y}_{pg})\}X_{MV}^* + \big\{2\big(\tilde{Z}_E^{0t} + \mu_S\tilde{Z}^t\big) - \cos\theta\,\tilde{Z}_{MS}^{pg}\big\}Y_{MV}^* + \big\{\big(\tilde{X}_{pp} - \tilde{Y}_{pp} - 2\mu_S\tilde{X}_{gg} + 2\mu_V\tilde{Y}_{gg} - 2\tilde{Z}_E^{0t} - 2\mu_S\tilde{Z}^t\big) + \cos\theta\big(\tilde{X}_{pg} - \tilde{Y}_{pg} - \mu_V\tilde{X}_{pg} + \mu_S\tilde{Y}_{pg} + \tilde{Z}_{MS}^{pg}\big)\big\}X_{MS}^* + 2\mu_S\tilde{Z}^{tg}Y_{MS}^*\big], \tag{A34}$$

$$c_x^{0s} = \frac{2}{\Sigma_{\rm PC}}\sin\theta{\rm Im}\big[-\big\{\tilde{Z}_{MV}^{pg} + \cos\theta\big(\tilde{Z}_E^{0s} + \mu_V\tilde{Z}^{sg}\big)\big\}(X_E^* - Y_E^*) + 2\big(\tilde{Z}_E^{0s} + \mu_V\tilde{Z}^{sg}\big)Y_{MV}^* - 2\big(\tilde{Z}_E^{0s} + \mu_V\tilde{Z}^{sg}\big)X_{MS}^*\big], \tag{A35}$$

$$c_x^{1} = \frac{2}{\Sigma_{\rm PC}}\sin\theta{\rm Im}\big[\big\{\tilde{Z}_{MS}^{pg} + \cos\theta\big(2\tilde{Z}_E^{1} + \mu_V\tilde{Z}^t - \mu_S\tilde{Z}^s - \mu_V\tilde{Z}^{tg}\big)\big\}(X_E^* - Y_E^*) - \big\{\big(\tilde{X}_{pp} - \tilde{Y}_{pp} + 2\mu_V\tilde{X}_{gg} - 2\mu_S\tilde{Y}_{gg} + 2\tilde{Z}_E^1 + 2\mu_V\tilde{Z}^t\big) + \cos\theta(\tilde{X}_{pg} - \tilde{Y}_{pg} + \mu_S\tilde{X}_{pg} - \mu_V\tilde{Y}_{pg})\big\}X_{MV}^* + \{-2\big(\tilde{Z}_E^1 - \mu_V\tilde{Z}^{tg} - \mu_S\tilde{Z}^s\big) + \cos\theta\,\tilde{Z}_{MS}^{pg}\big\}Y_{MV}^*\big\{\big(\tilde{X}_{pp} - \tilde{Y}_{pp} - 2\mu_S\tilde{X}_{gg} + 2\mu_V\tilde{Y}_{gg} + 2\tilde{Z}_E^1 - 2\mu_V\tilde{Z}^{tg} - 2\mu_S\tilde{Z}^s\big) + \cos\theta(\tilde{X}_{pg} - \tilde{Y}_{pg} - \mu_V\tilde{X}_{pg} + \mu_S\tilde{Y}_{pg} + 2\mu_S\tilde{X}_{pg} - 2\mu_V\tilde{Y}_{pg} - \tilde{Z}_{MS}^{pg})\big\}X_{MS}^* + 2\big(\tilde{Z}_E^1 + \mu_V\tilde{Z}^t\big)Y_{MS}^*\big]. \tag{A36}$$


[1] B. Desplanques, J. F. Donoghue, and B. R. Holstein, Ann. Phys. (NY) **124**, 449 (1980).
[2] C. H. Hyun, T.-S. Park, and D.-P. Min, Phys. Lett. B **516**, 321 (2001).
[3] R. Schiavilla, J. Carlson, and M. W. Paris, Phys. Rev. C **70**, 044007 (2004).
[4] C. H. Hyun and B. Desplanques, Phys. Lett. B **552**, 41 (2003).
[5] C.-P. Liu, C. H. Hyun, and B. Desplanques, Phys. Rev. C **68**, 045501 (2003).
[6] S. Ahmad, S. K. Singh, and H. Arenhövel, Eur. Phys. J. A **40**, 151 (2009).
[7] C. H. Hyun, S. J. Lee, J. Haidenbauer, and S. W. Hong, Eur. Phys. J. A **24**, 129 (2005).
[8] C.-P. Liu, C. H. Hyun, and B. Desplanques, Phys. Rev. C **69**, 065502 (2004).
[9] M. Fujiwara and A. I. Titov, Phys. Rev. C **69**, 065503 (2004).
[10] C. H. Hyun, C.-P. Liu, and B. Desplanques, Eur. Phys. J. A **24**, 179 (2005).
[11] C.-P. Liu, C. H. Hyun, and B. Desplanques, Phys. Rev. C **73**, 065501 (2006).
[12] B. Desplanques, C. H. Hyun, S.-I. Ando, and C.-P. Liu, Phys. Rev. C **77**, 064002 (2008).
[13] P. D. Eversheim *et al.*, Phys. Lett. B **256**, 11 (1991).
[14] V. A. Knyazkov *et al.*, Nucl. Phys. A **417**, 209 (1984).
[15] M. T. Gericke *et al.*, Phys. Rev. C **83**, 015505 (2011).
[16] S. L. Zhu, C. M. Maekawa, B. R. Holstein, M. J. Ransey-Musolf, and U. van Kolck, Nucl. Phys. A **748**, 435 (2005).
[17] L. Girlanda, Phys. Rev. C **77**, 067001 (2008).
[18] M. J. Savage, Nucl. Phys. A **695**, 365 (2001).
[19] C. H. Hyun, S. Ando, and B. Desplanques, Phys. Lett. B **651**, 257 (2007).
[20] C.-P. Liu, Phys. Rev. C **75**, 065501 (2007).
[21] D. R. Phillips, M. R. Schindler, and R. P. Springer, Nucl. Phys. A **822**, 1 (2009).
[22] J. W. Shin, S. Ando, and C. H. Hyun, Phys. Rev. C **81**, 055501 (2010).
[23] M. R. Schindler and R. P. Springer, Nucl. Phys. A **846**, 51 (2010).
[24] M. L. Rustgi, W. Zernik, G. Breit, and D. J. Andrews, Phys. Rev. **120**, 1881 (1960).
[25] H. Arenhövel and M. Sanzone, Few Body Syst. Suppl. **3**, 1 (1991).
[26] K. M. Schmitt, P. Wilhelm, and H. Arenhövel, Few Body Syst. **10**, 105 (1991).
[27] R. Schiavilla, Phys. Rev. C **72**, 034001 (2005).
[28] V. I. Kukulin, I. T. Obukhovsky, V. N. Pomerantsev, A. Faessler, and P. Grabmayr, Phys. Rev. C **77**, 041001(R) (2008).
[29] S.-I. Ando, Y.-H. Song, C. H. Hyun, and K. Kubodera, Phys. Rev. C **83**, 064002 (2011).
[30] S. I. Ando and C. H. Hyun, Phys. Rev. C **72**, 014008 (2005).
[31] S. Ando, R. H. Cyburt, S. W. Hong, and C. H. Hyun, Phys. Rev. C **74**, 025809 (2006).
[32] S. Ando, J. W. Shin, C. H. Hyun, S. W. Hong, and K. Kubodera, Phys. Lett. B **668**, 187 (2008).
[33] S. R. Beane and M. J. Savage, Nucl. Phys. A **694**, 511 (2001).
[34] J. Alberi *et al.*, Can. J. Phys. **66**, 542 (1988).
[35] S.-I. Ando and C. H. Hyun, Phys. Rev. C **86**, 024002 (2012).
[36] C.-P. Liu and C. H. Hyun (unpublished).